# VCSEL Laser System for Atomic Clocks

Nathan Belcher *REU program, College of William and Mary*
I. Novikova *College of William and Mary, Physics Department*

August 3, 2007

**Abstract**

Working with a vertical-cavity surface-emitting laser (VCSEL), I am studying its properties with phase modulation and testing its known characteristics. A VCSEL made by Roithner was found to have two orthogonal polarizations and the ability to modulate a one-to-one sideband to carrier ratio at 6.834 GHz but lased at 775 nm, which was too low to be used in finding resonances in rubidium. With a VCSEL made by Ulm, a single mode was seen at all times, one-to-one sideband to carrier modulation occured at 6.834 GHz, resonances were found at 794.7 nm.

## 1 Introduction

In the last decade, advances have been made in creating miniature (sub-cubic centimeter) atomic clocks, based on laser probing of a vapor. The laser employed in these clocks is a vertical-cavity surface-emitting laser (VCSEL), which has useful characteristics for this application. The overall goal of my project is to create a prototype atomic clock, and this summer's research has been all about lasers. The VCSEL is a type of diode laser that has its lasing medium vertical, instead of horizontal like other diode lasers. VCSELs are studied because of their low power consumption, ease of current modulation with rf signals, and use in miniature atomic clocks. This paper will describe the theory behind VCSEL modulation, the hardware necessary to temperature stabilize, provide current, measure the characteristics of the VCSEL, and the data and results seen during the summer's research.

# 2 Theory

While the focus of the research has been on the VCSELs, the theory for the prototype atomic clock is driving the research. Therefore, understanding the theory behind the atomic clocks will allow the research to become more focused and provide solutions to problems found in the research. The atomic clocks contain three parts: a transition in an alkali metal atom (that has free valence electrons), a frequency modulator with counter, and a laser. The element of use in this atomic clock is rubidium, which has one free valence electron. The frequency modulator provides phase modulation, creating two electro-magnetic fields at different frequencies out of one physical laser. A counter matches the frequency driven by the modulator to give a reference for time, and the laser drives the entire process.

## 2.1 Transitions in Rubidium

In the rubidium electron energy levels, the transition wavelengths used in this atomic clock are 780 nm or 794.7 nm. These match the transitions from $5S_{1/2}$ to $5P_{3/2}$ and $5P_{1/2}$ respectively, and the hyperfine splitting at 6.834 GHz is contained in the $5S_{1/2}$ energy level. Hyperfine splitting is a correction to the energy levels due to the difference in the spin orientation of the nucleus with the spin of the electrons, and is a small correction. The three level system comprised of two $5S_{1/2}$ hyperfine states and either the $5P_{3/2}$ or $5P_{1/2}$ levels forms what is known as a lambda system (figure 1). It is called a lambda system because of the resemblence to the Greek capital $\Lambda$, and the X represents an electro-dipole forbidden transition in the system. $\omega_c$ is the carrier frequency the laser must match to raise the electrons into the excited state, while $\omega_p$ (probe frequency) is the carrier frequency plus the hyperfine splitting frequency.

When the laser drives the electrons into the excited state, some will decay into the hyperfine split level denoted by state 1 in the figure. In a process called electromagnetically induced transparency, all of the electrons will be driven to the quantum superposition of states 1 and 2 (a "dark" state), which does not interact with either electromagnetic field causing the atomic sample to become transparent. This transparency happens only if a frequency difference between $\omega_c$ and $\omega_p$ is very close to the hyperfine splitting between states 1 and 3 (clock transition), and allows the locking of a frequency modulator to the counter at the clock frequency.

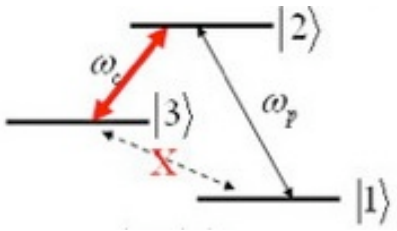


Figure 1: A lambda system. Levels 1 and 3 are states in $5S_{1/2}$ seperated by the hyperfine splitting (6.834 GHz), and level 2 is 780 or 794.7 nm away from the $5S_{1/2}$ state.

## 2.2 Phase Modulation

Because the lambda system needs two different frequencies of laser light, a few problems exist. The first problem is the laser will move around a set frequency in a random way ("jump"), regardless of the quality of the laser. If two physically seperate lasers are used at two different frequencies, they will both jump randomly and not have any correlation. To alleviate this problem, phase modulation is used to create two lasers out of one physical laser. Even through there will still be jumps around the set frequency, both lasers will jump in the same way. The relative frequency of the two lasers can be set by an external generator, and this creates a carrier with sideband comb.

The mathematics behind phase modulation are useful, so I will explain them. A generic wave is created with the form

$$E = E_0 e^{ikx - i\omega t + i\varphi(t)} \tag{1}$$

where $E_0$ is the amplitude of the wave and $\omega$ is the phase. $\varphi$(t) is the modulation wave in the form

$$\varphi(t) = \varepsilon sin(\omega_m t) \tag{2}$$

where $\varepsilon$ is the amplitude of modulation and $\omega_m$ is the modulation frequency. Combining the two equations gives

$$E = E_0 e^{ikx - i\omega t + i\varepsilon sin(\omega_m t)} \tag{3}$$

To decompose this equation into amplitude and frequency parts, Bessel func-

tions must be used. From the generic Bessel function equation

$$e^{insin(\varphi m)} = \sum_{n=0}^{\infty} J_n(\varepsilon) e^{im\varphi} \tag{4}$$

the i$\varepsilon$sin($\omega_m$t) of equation 3 can be broken into

$$e^{in\varepsilon sin(\omega_m t)} = \sum_{n=0}^{\infty} J_n(\varepsilon) e^{i\omega_m nt} \tag{5}$$

Substituting equation 5 into equation 3 gives

$$E = \sum_{n=0}^{\infty} E_0 J_n(\varepsilon) e^{ikx - i\omega t + i\omega_m nt} \tag{6}$$

and rearranging shows the final form

$$E = \sum_{n=0}^{\infty} E_0 J_n(\varepsilon) e^{ikx - i(\omega - n\omega_m)t} \tag{7}$$

This equation is the basis for the carrier and sideband comb, because the frequency difference between the carrier and each nth sideband is determined by $\omega$-n$\omega_m$.

An advantage of using the VCSELs is that their output can be phase-modulated by direct current modulation. This allows matching of the hyperfine splitting in the rubidium vapor, because the frequency difference can be chosen. In additon, the amplitude of the sidebands and carrier are determined by the nth-order Bessel function and can be calculated.

# 3 Hardware

## 3.1 Temperature Stability

Because the project started from the beginning, we had complete control over the design and fabrication of the hardware for the laser system. Using ideas from Sergey Zibrov at Lebedev Physics Institute in Russia, who had designed a temperature controlled diode laser system, a system was created that would be robust yet easily assembled and disassembled when changing

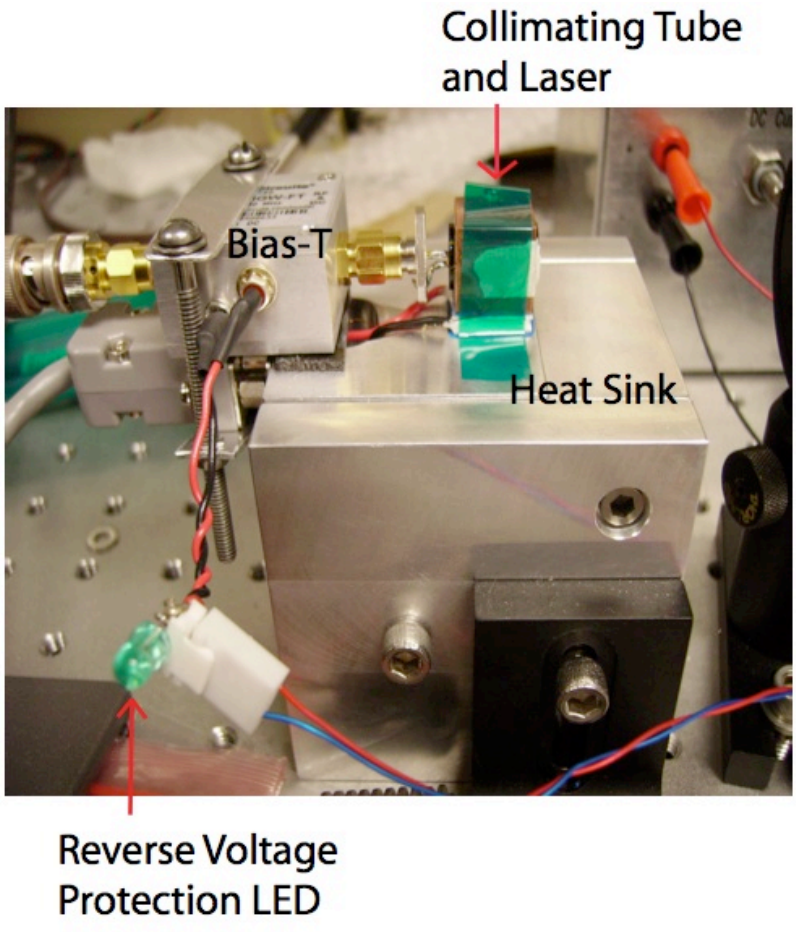


Figure 2: The laser system.

laser diodes. The laser needed to be held at a fixed temperature to achieve stability in wavelength, so the system was designed to keep the laser at a given temperature.

Figure 2 shows the laser system designed by our group. The system provides the laser with a stable temperature and modulation of the laser's current, which are both necessary in the prototype atomic clock. The basis for the laser system is the heat sink, which doubles as the holding block for the system. The temperature controller uses a peltier that heats or cools depending on the direction of current flow, and the peltier needs a large piece of metal from which to draw or give heat. This large piece of aluminum was

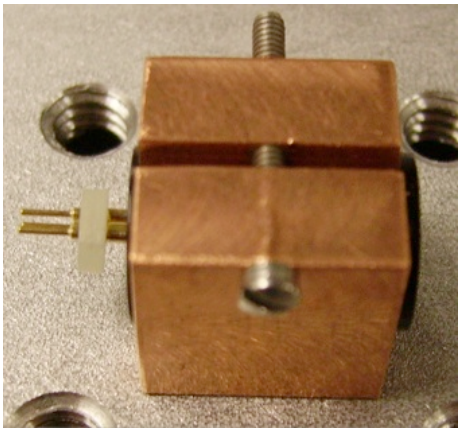

Figure 3: Collimating tube holder for the lasers. The laser is installed on the left hand side and lases to the right.

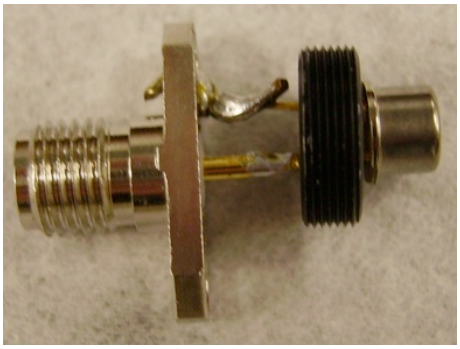

Figure 4: VCSEL diode with SMA connector. The black piece is a screw that holds the laser in the collimating tube.

also designed with a piece to be raised or lowered, allowing a changing beam height.

Using a temperature conducting epoxy, a copper block containing the collimating lens and diode holder for the laser (figure 3) was placed on the peltier. This block was made from copper because it can change temperature relatively quickly and gives the laser a stable basis from which to heat or cool. The laser is installed on the left side of the picture (with the three pin connector) and lases towards the right of the picture. There were difficulties with the collimating lens, because the size of the diode cap did not allow the collimating lens to reach its focal point. Another lens had to be ordered with a longer focal length, and this lens was able to collimate the beam.

The temperature contoller drives the peltier, and was purchased from Wavelength Electronics, Inc. (model number WTC3293-14000). The temperature can be set using a potentiometer from 0 to 70 degrees Celsius, but it has been found that the peltier can only drive the temperature to about 37 degrees Celsius due to a current limit of 0.5 A. The controller is stored in a box with a cutout for a D-sub connector and LED screen, and is connected to the peltier and thermistor through another D-sub connector mounted on the heat sink.

The SMA on the laser (figure 4) is connected to the Bias-T, which mixes rf modulation and dc current and outputs to the laser. The rf signal is input to

the Bias-T by a digital synthesizer, which produces rf power at very accurate frequencies, and the dc current is provided by a constant current source.

In addition to the pieces shown, there is also a metal box with a hole for the laser that is placed on top of the heat sink and around the collimating tube holder. This stabilizes the air around the laser, because the small airflow in the laboratory is enough to cause temperature fluctuations large enough to affect the wavelength of the laser. The temperature fluctuations are especially noticable when operating at temperatures above 35 degrees Celsius.

## 3.2 Lasers

The group has experimented with four diodes: ThorLabs 780 nm diode laser, ThorLabs 780 nm VCSEL, Roithner 780 nm VCSEL, and Ulm 794 nm VCSEL. The diode is installed into the collimating tube and attached to an SMA connector (figures 3 and 4), which allows transfer of high-frequency rf signals with little loss. The leads of each laser are cut short to minimize picking up unwanted stray signals and losses in the connectors. Three of the four types of lasers are in the TO46 package, as seen in figure 4, and all have a head size within .1 mm of 5.5 mm. The following table shows some characteristics of each type of laser, and the data and results collected from each laser will be explained in the Data and Results section.

Table 1: The four lasers tested and characteristics.

| Laser | Type | $\lambda$ (Spec. Sheet) | $\lambda$ (Measured) | Max. Current | Max. Power | Package |
|---|---|---|---|---|---|---|
| ThorLabs | Regular Diode | 780 nm | - | 70 mA | 10 mW | TO-18 |
| ThorLabs | VCSEL | 780 nm | 775 nm | 8 mA | 1.65 mW | TO46 |
| Roithner | VCSEL | 780 nm | 775 nm | 8 mA | 1.87 mW | TO46 |
| Ulm | VCSEL | 795 nm | 794 nm | 3 mA | 500 $\mu$W | TO46 |

## 3.3 Power Supplies

To provide the laser with current, three power supplies have been used. The first attempt at providing current was with an ILX Lightwave constant current supply, but this power supply produced too much noise in the output

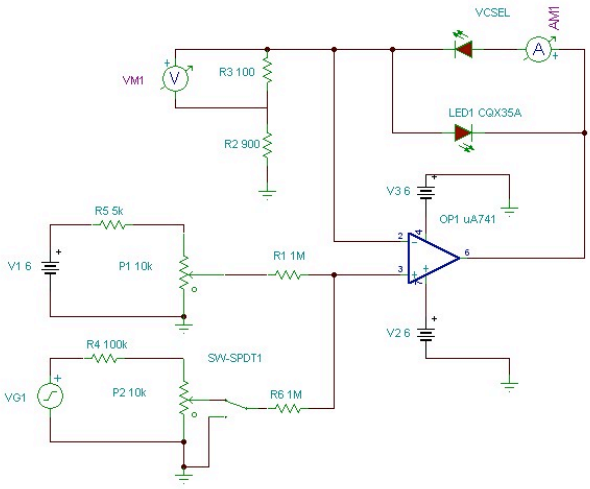


Figure 5: The schematic for the first battery-powered constant current supply.

signal at low currents (less than 10 mA). Because no other commercially sold power supply was available, a switch was made to battery-powered constant current sources. The first power supply fabricated had a simple circuit design, with no built-in protection against high reverse voltages or exceeding the maximum forward current. The user had to be aware of the dc and low frequency modulated current (from a function generator) into the laser at all times.

After destroying an Ulm VCSEL by exceeding the reverse voltage (no light emitted when current input to laser), the first power supply was retired for the second battery-powered constant current supply. This power supply was fabricated with more developed circuitry to provide protection for the laser from exceeding the maximum reverse voltage and maximum forward current. Unfortunately, the first circuit design (figure 5) had the laser in feedback of an operational amplifier on floating ground, and when the Bias-T was grounded the laser shorted. This caused a massive forward current through the laser, destroying the second Ulm VCSEL. The symptoms of exceeding the forward current are a decrease in the laser power and a major shift in wavelength (the wavelength went to approximately 760 nm with 3 $\mu$W of power from 794 nm with 350 $\mu$W of power). Also, the laser will turn on immediately when current is provided, instead of having a lasing threshold. The second

attempt at a protection circuit (figure 7) should provide proper protection for the laser, and has been tested with the ThorLabs VCSEL.

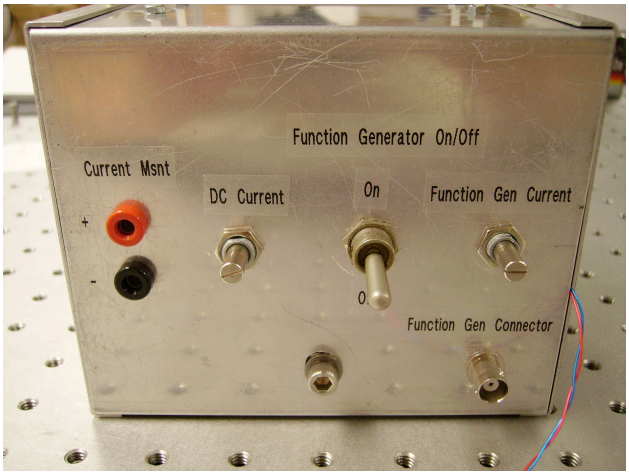


Figure 6: The second battery-powered constant current supply.

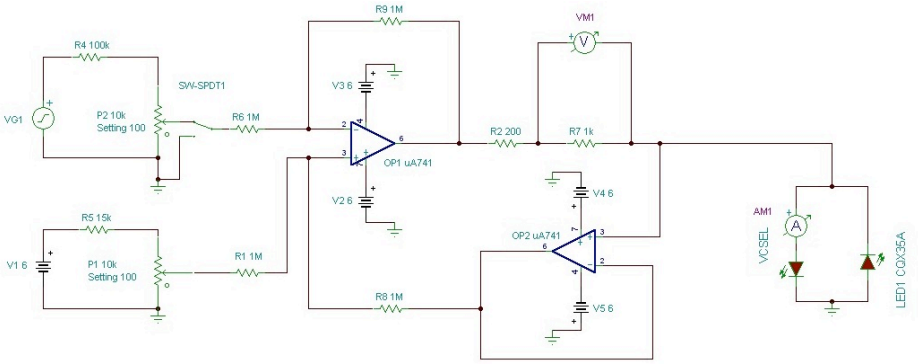


Figure 7: The schematic for the second battery-powered constant current supply.

## 3.4 Measuring Setups

After the laser has been installed in the laser system, measurements are taken to see modulation, polarization, and resonances in rubidium. Modulation and

polarization use the same optical setup, while the resonances in rubidium use a different optical setup.

To see signal that has meaning for phase modulation, an interferometer (Fabry-Perot cavity) must be used. A Fabry-Perot cavity is a set of two mirrors with 99 percent reflectivity aligned such that the mirrors are parallel with each other and perpindicular with the beam (see figure 8). When this alignment is achieved, the waves reflecting off the mirrors constructively interfere to create transmission through the mirrors. For the early measurements of the Roithner VCSEL modulation, a purchased Fabry-Perot cavity with length of 5 cm and a free spectral range (FSR) of 1.5 GHz was used. This FSR was not enough to see the full effect of rf modulation, so a cavity with a length of approximately 5 mm was created from two mirrors. We achieved an FSR of approximately 40 GHz and a finesse of approximately 100, which allowed resolution of second and third sidebands.

This Fabry-Perot cavity was fabricated by epoxying two piezoelectric crystals on a lens mount (see figure 8; the piezos are the green pieces on the top mirror) and connecting their wires to a BNC connector. Piezoelectric crystals work by changing the length of the crystaline structure in one plane based on the input voltage, and the BNC connector was attached to a piezo scanner (made by ThorLabs) which provided an input voltage. The piezo scanner was modulated with a function generator to provide scanning of the length of the cavity, providing transmission of the wave through the cavity and giving a signal on the oscilloscope.

Alignment of the Fabry-Perot cavity has proven difficult with the low powered lasers, because of the decrease in signal after the cavity. To align the cavity, an iris is placed after the optical isolator (see figure 9) to indicate the position of the reflection. The mirror with the piezoelectric crystals (see figure 8) is installed on the optical table, and its reflection is moved with screws on the optical mount to be directly back into the iris. The front mirror is then installed, and its reflection is also moved back into the iris. Both mirrors reflections are moved into the iris to crudely align the mirror to each other and to the incident beam, and fine-tuned to each other and the photodetector with the screws on the mirror mounts.

For the modulation and polarization measurements, either the Fabry-Perot cavity or the current into the laser could be scanned. Using the optical setup in figure 9, the modulation figures in the Data and Results were taken by scanning the Fabry-Perot cavity. When the polarizations were observed with the Roithner VCSEL, the input current to the laser was scanned with

a triangle wave from a function generator. The Fabry-Perot cavity was still used to see the signal, but the piezoelectrics were not scanned.

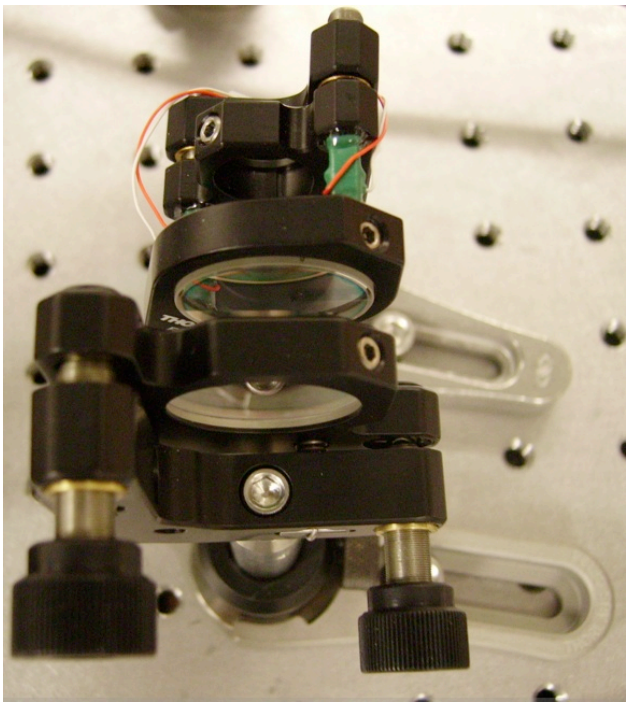

Figure 8: The Fabry-Perot cavity with length of approximately 5 mm.

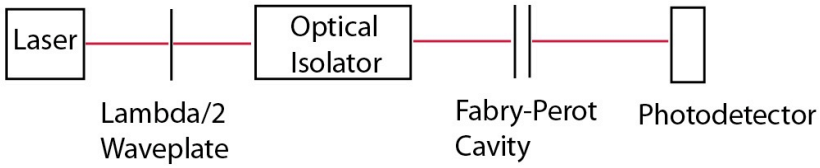


Figure 9: Visual schematic of optical setup for measurement of polarizations and modulation.

To measure the rubidium resonances in a rubidium vapor cell, the optical setup in figure 10 was used. The input current of the laser was modulated by a function generator, and the output measured by the oscilloscope. When we first saw the resonances, they just looked like noise at the top of the triangle wave. But, as the current was increased, we saw the "noise" (resonances)

move down the triangle wave. When the vapor cell was taken out, the input triangle wave was seen without noise, causing us to understand that the noise seen on the triangle wave was in fact the resonances of rubidium.

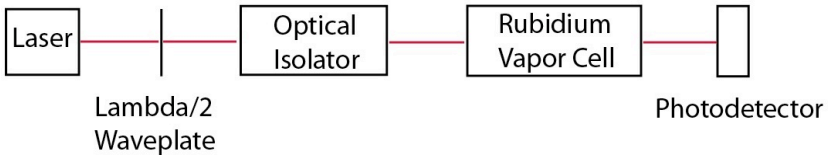


Figure 10: Visual schematic of optical setup for measurement of rubidium resonances.

# 4 Data and Results

To be used in the prototype atomic clock, each laser must meet three qualifications. First, the laser must operate on a single mode; second, the laser must have strong phase modulation (close to one-to-one sideband to carrier ratio at 6.834 GHz); and third, the laser must tune to an atomic transition in rubidium. All four lasers mentioned previously have been tested, and the results are as follows: The ThorLabs diode laser did not meet the modulation or tunability requirements, because modulation only occured up to 2 GHz. Also, the bandwidth of the laser was approximately 100 MHz, which is too wide for use in the clock. The ThorLabs VCSEL failed the single mode, modulation, and tunability requirements, allowing this laser to be used as the test diode for the improved protection circuit (if it died, it didn't matter!).

The Roithner VCSEL met the requirement for modulation, failed the tunability requirement, and met the requirement for single mode at low input currents. As will be explained in further depth in the Roithner VCSEL section, at higher currents two orthogonal polarizations mixed, producing undesired results. Much work had been done with the Roithner VCSEL (polarization and modulation measurements) before the wavelength was measured, and we had hoped the laser would tune to the resonances. The results with this laser are still valid, and could be useful if a laser was found to have an initial wavelength closer to 780 nm.

The Ulm VCSEL is the only laser to meet all three requirements, and was installed in the laser system to see resonances in rubidium. The first

Ulm VCSEL installed had an initial wavelength of 794 nm and lased with approximately 420 $\mu$W of power, and the second Ulm VCSEL had an initial wavelength of 792.9 nm with approximately 285 $\mu$W of power. Further results will be discussed in the Ulm VCSEL section.

## 4.1 Roithner VCSEL

While the Roithner VCSELs failed the tunability requirements, this was not found until much work characterizing these lasers had been completed (the optical multimeter did not arrive for some time). This laser was the first understanding of phase modulation in VCSELs, and the characterization of the two orthogonal polarizations provided interesting results.

After installing the VCSEL and connecting to the digital sythnesizer, several attempts were made to modulate the VCSEL. With the long Fabry-Perot cavity, modulation at 3.4 and 6.8 GHz was observed and data collected. The sideband to carrier ratio approached 1 for both modulation frequencies, at approximately 4.6 dBm of power for 3.4 GHz and 8.1 dBm for 6.8 GHz (see figures 11 and 12). After switching to the short Fabry-Perot cavity, more data was taken. As seen in figures 13-15, the sideband to carrier ratio for 6.8 GHz increases from 5 percent at 6 dBm to 97 percent at 14 dBm.

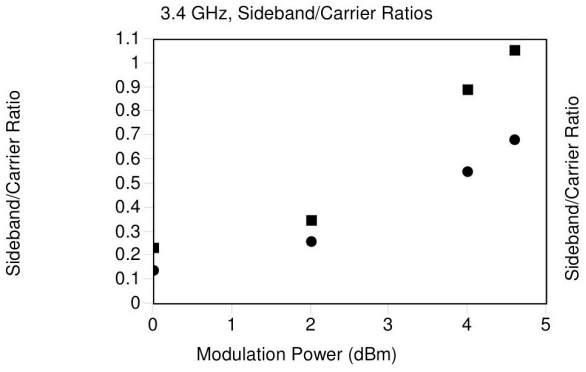


Figure 11: The left and right sideband-to-carrier ratios for 3.4 GHz modulation frequency.

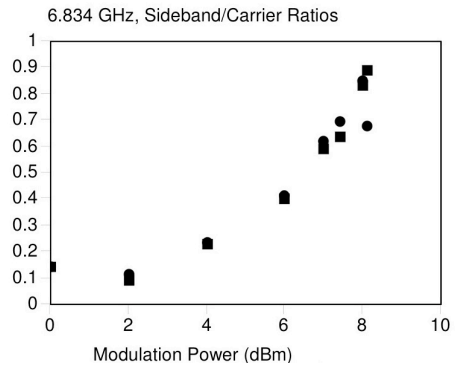


Figure 12: The left and right sideband-to-carrier ratios for 6.8 GHz modulation frequency.

One interesting result found centered on the "saturation" of the signal on the oscilloscope based on the modulation frequency and current. Saturation of the signal occurred when there were too many sidebands with not enough

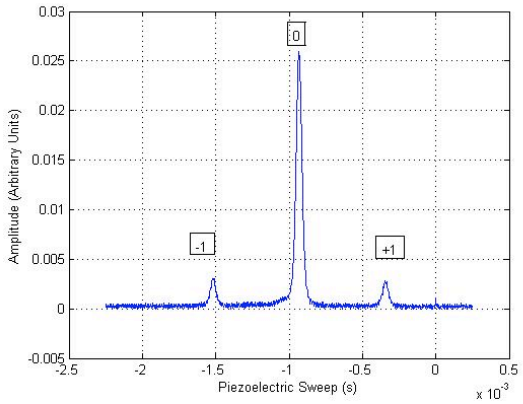


Figure 13: Modulation of the Roithner VCSEL at 6.8 GHz and 5 dBm of power.

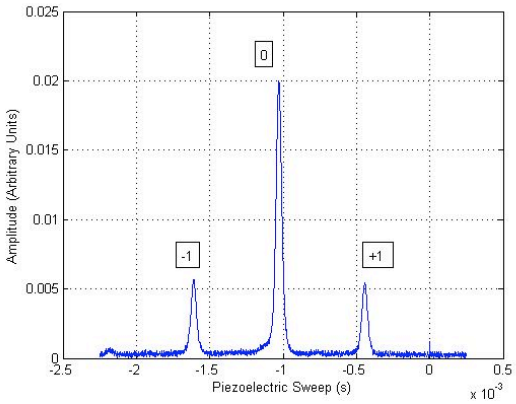


Figure 14: Modulation of the Roithner VCSEL at 6.8 GHz and 9 dBm of power.

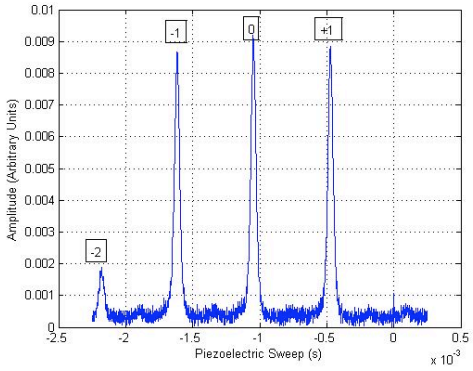


Figure 15: Modulation of the Roithner VCSEL at 6.8 GHz and 14 dBm of power.

energy in each, causing a drop of the signal from sharp, high peaks to wide, low peaks barely above the noise on the scope. We found that the saturation depended strongly on input current for modulation at 3.4 GHz, but was almost independent for modulation at 6.8 GHz. The sideband to carrier ratio at 3.4 GHz decreased from 500 percent at 1.90 mA to 10 percent at 2.80 mA, but the sideband to carrier ratio at 6.8 GHz increased from 30 percent at 1.90 mA to 60 percent at 2.80 mA.

The polarizations of the Roithner laser also produced interesting results. We found two orthogonal polarizations that could be seperated with a $\lambda/2$ waveplate at currents less than 2 mA, but mixed with currents over 2 mA. In figure 16, the blue signal represents the first polarization, the green represents the second polarization, and the wave shape is triangular from a function generator. When the laser reaches its threshold, it lases on the first polarization and not the second. As the current is swept, the laser switches to the second polarization, extinguishing the first. In each of these two locations, turning the waveplate to the opposite polarization causes a loss of signal on the oscilloscope. When the current is increased above the single mode regime (figure 17, again with a triangular input from a function generator), the laser operates on both polarizations. Lasing on the first polarization directly after the threshold is still seen, but the the blue signal after the second polarization lases (green signal) indicates lasing of both polarizations. At this current, turning the waveplate changes the signal on the oscilloscope from one polarization to the other, but does not extinguish either one.

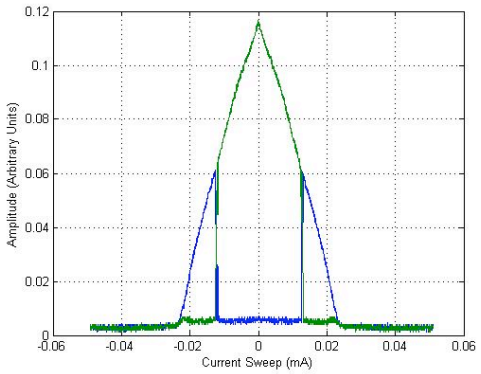


Figure 16: Two orthogonal polarization of the Roithner VCSEL at 1.35 mA.

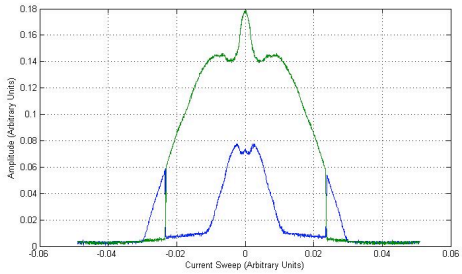


Figure 17: Two orthogonal polarizations of the Roithner VCSEL at 2.09 mA.

The Roithner VCSEL was the first attempt to find resonances in rubidium and be modulated at 6.8 GHz, but the wavelength measurement equipment did not arrive until after some modulation and polarization work had been done. When the optical multimeter was received, the measurement of the installed VCSEL was completed. The lasers were rated for 780 nm, but we found two of the five lasers to have a wavelength of 857 nm. After switching to

a laser close to 780 nm, we took measurements of the wavelength. We found that the laser had a wavelength of 775 nm at room temperature, and tried to increase the temperature to increase the wavelength. The laser is rated for 0.06 $\Delta\lambda/\Delta T$, which was found to be consistent with the test conducted. We concluded that to reach the resonances of rubidium, the Ulm VCSEL would have to be used in the experimental setup.

## 4.2 Ulm VCSEL

When the Ulm VCSELs arrived, the three requirements for use in the protype atom clock were checked. The first test was wavelength to see how close the lasers were to rubidium resonance. The Ulm VCSELs are rated for 795 nm $\pm$ 1 nm, and the wavemeter showed that the actual wavelength at room temperature was 794 nm. With Ulm VCSEL 1, resonance was seen at 36.4 degrees Celsius and 1.70 mA of current (figure 18).

The Ulm VCSELs also meet the other two requirements of single mode and modulation. These lasers operate at a single mode for the entire current range, and can be modulated to 6.8 GHz with a one-to-one sideband to carrier ratio at 13 dBm. Because these lasers possess the same modulation characteristics as the Roithner VCSELs, we have a good understanding of how the laser will operate when modulated.

After seeing resonances in the rubidium, we ran into a bit of trouble. As explained in the Power Supplies subsection of the Hardware section, the first constant current source did not have any reverse voltage protection. I input too much reverse voltage when testing the resonance of the Ulm 1 with the first current box and destroyed the lasing cavity. The symptom of destroying the lasing cavity is that no light will be emitted from the laser when current is input, and this is what was seen. From this, it was determined that protection for the VCSELs was needed, and the second current box was fabricated.

After installing the Ulm VCSEL 2 into the system with the second current box, resonances were seen again. Ulm VCSEL 2 had an initial wavelength of 792.9 nm, and required an extra resistor providing heat onto the copper block that holds the laser. A temperature of 40.6 degrees Celsius and 1.9 mA were used to see the resonances (figure 19). Again, unfortunately, the Ulm VCSEL was broken, this time by too much forward current. As explained in the Power Supplies subsection of the Hardware section, the circuit shorted to ground and provided approximately 10 mA through the laser. This certainly exceeded the 3 mA absolute maximum rating, and caused the second Ulm to

stop lasing. When more Ulm VCSELs arrive, resonances will be found and we will attempt to see electromagnetically induced transparency.

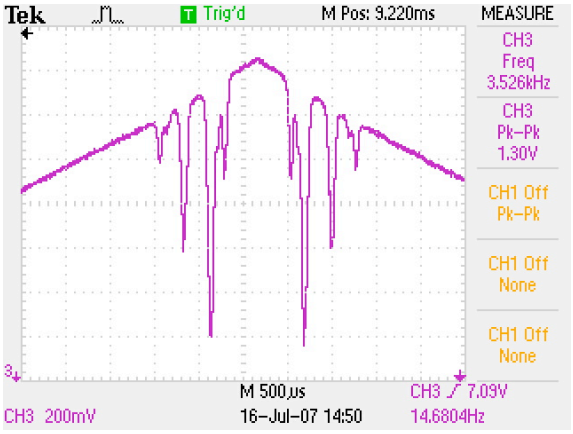


Figure 18: Rubidium resonances using the first Ulm VCSEL at 794.7 nm.

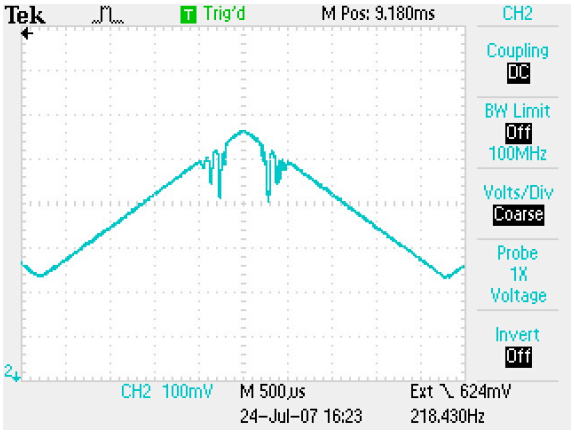


Figure 19: Rubidium resonances using the second Ulm VCSEL at 794.7 nm.

# 5 Conclusion

After testing the Roithner and Ulm VCSELs, there is a better understanding of how the VCSELs perform. A one-to-one sideband to carrier ratio at 3.4 and 6.8 GHz has been achieved with the Roithner VCSELs, and the Ulm VCSELs show the same modulation characteristics. Resonances were also seen with the Ulm VCSELs, and when more arrive further testing of the resonances will begin to see electromagnetically induced transparency.

# 6 Acknowledgements

I would like to thank Profossor W. J. Kossler and the REU program at The College of William and Mary, sponsored by NSF REU Grant number PHY-0453502. Also, I thank Professor Irina Novikova for allowing me to work in her laboratory and guiding me through this research and Professor Eugeniy Mikhailov for his electronic help.